RESEARCH PAPER

Effects of *Cinnamomum zeylanicum* Against Hydroxychloroquine-Induced Toxicity to address Drug-induced Cardiotoxicity

Priyadarshini Gupta and Vibha Rani*
E-mail address: vibha.rani@jiit.ac.in (Corresponding author)
priyadarshinigupta23@gmail.com (First author)
Transcriptome laboratory, Centre of Emerging Diseases, Department of Biotechnology, Jaypee Institute of Information Technology, A-10, Sector-62, Noida, Uttar Pradesh, India 201309
***Corresponding author**
Transcriptome Laboratory, Centre of Emerging Diseases, Department of Biotechnology,
Jaypee Institute of Information Technology,
A-10, Sector-62, Noida, Uttar Pradesh, India
Tel.: +91 1202594210; Fax: +91 1202400986

Abstract
Drug-induced toxicity is a serious concern and exploring the efficacy of natural products having cardioprotective properties could offer a valuable therapeutic strategy to mitigate the risk of cardiotoxicity while maintaining the drug efficacy. The present study aimed to analyze the efficacy of the *Cinnamomum zeylanicum* (CZE) ethanolic extract of bark in HCQ-induced cardiotoxicity. Biochemical and Structural screening of Bioactive compounds was examined using HPLC and FTIR spectroscopy. The antiradical activity was assessed using DPPH (2,2-diphenyl-1-picrylhydrazyl) assay. DCFH-DA confirmed the intracellular free radical levels in experimental sets. Furthermore, the Hoescht/MitoTracker Red and Ethidium bromide/Acridine Orange dual staining method and flow cytometric analysis confirmed apoptosis as the primary mechanism of HCQ-induced cardiotoxicity synergistically mitigated by *C. zeylanicum*. The HPLC and FTIR findings revealed the abundant presence of flavonoids and phenolic compounds. DPPH analysis showed a strong antioxidative potential with the increasing CZE concentration. DCFH-DA exhibited a significant decrease in intracellular free radical scavenging activity. Hoescht and MitoTracker red staining showed a decrease of mROS when treated with CZE. EtBr/AO staining revealed the reversal of late apoptosis to early apoptosis. A decrease in apoptotic cells was observed in co-treated cells using flow cytometric analysis. Recent research demonstrates that chronic HCQ usage could trigger the formation of oxidative stress and ROS, which can further lead to arrhythmias, hypertension, and serious cardiac problems. Moreover, the generation of oxidative stress can potentially induce nuclear deformation indicative of cellular dysfunction. Our study suggests the potential application of *C. zeylanicum* bark extract as an antioxidant and cardioprotective. Moreover, the medicinal attributes of the plant reflect the synergism among different phytochemicals in the nutraceutical and phytopharmaceutical industries.

Keywords: *Cinnamomum zeylanicum*, Functional food, Anti-inflammatory, Cardioprotective, toxicity, Phytotherapeutics
How to cite this article: Priyadarshini Gupta and Vibha Rani*. Effects of Cinnamomum zeylanicum Against Hydroxychloroquine-Induced Toxicity to address Drug-induced Cardiotoxicity. Int J Drug Deliv Technol. 2026;16(77s):946-958. DOI: 10.25258/ijddt.16.77s.110.

Introduction

With the paradigm shift in the field of nutritional philosophy, functional foods have gained interest in both scientific and public domains for their potential health benefits. Functional foods offer health advantages beyond fundamental nutritional value with abundant bioactive compounds positively elevating overall body functions [1]. These are enriched with phytoconstituents such as tannins, polyphenols, alkaloids, and flavonoids with the potential to inhibit cellular pathways and events related to proliferation, communication, and apoptosis in diseased conditions [2, 3]. With the variety of Functional foods available, *Cinnamomum zeylanicum* (commonly known as cinnamon) is a widely used culinary spice for its medicinal and therapeutic benefits.

Cinnamon (Family, Lauraceae) is a tree native to Southern India that has been traditionally used in various cultures for its aroma, flavour and therapeutic properties [4]. Ethnobotanical investigations have identified multiple bioactive constituents in cinnamon, including cinnamaldehyde, catechins, quercetin, procyanidins and cinnamic acid, which exhibit a range of biological activities [5]. These compounds have shown potential in modulating several pathophysiological processes, including anti-inflammatory, antioxidant, antidiabetic and antimicrobial effects [6]. Among its myriads of promising health benefits, cinnamon's bioaccessibility and bioavailability have recently come into focus. Histopathological studies suggest the hepatoprotective role of the bioactive compounds found in *C. zeylanicum* could be crucial in protecting against CCl_4-induced hepatotoxicity in rats [7].

Drug-induced toxicity is a significant concern in modern medicine, especially as certain medications, while therapeutically effective, can cause unintended damage to various organs. These toxic effects can emerge as a result of long-term usage or high dosages, often leading to serious complications. Hydroxychloroquine (HCQ) is an anti-malarial drug and has also been used for rheumatological diseases for ages. Given the recent outbreak of COVID-19, HCQ has emerged to be a possible candidate as a repurposed anti-viral drug [8]. Hydroxychloroquine has been linked to toxic effects with structural and functional impairment in different tissues, including the eyes, muscles, and heart, especially with prolonged use [9]. Among these, hydroxychloroquine-induced cardiotoxicity has gained attention due to its potentially severe implications [10].

Research indicates that HCQ-induced cardiotoxicity can manifest in various forms, including arrhythmias, cardiomyopathy, and conduction disorders. This toxicity is most commonly observed in patients on long-term HCQ therapy or those receiving higher-than-recommended doses and can lead to conditions like cardiomyopathy or conduction disorders [11]. The mechanisms underlying this toxicity involve disruptions in cardiac ion channels, leading to altered electrical activity, and accumulation of the drug in lysosomes within myocardial cells, causing cellular dysfunction [12]. Prolonged exposure to HCQ is linked to the generation of oxidative stress, mitochondrial damage, impaired autophagy, apoptosis, and inflammation in cardiac tissues, leading to heart failure, arrhythmias, and myocardial infarction. Additionally, HCQ extends the period of the QT interval, expanding the probability of severe arrhythmias like Torsades de Pointes. [13]. Therefore, HCQ-induced cardiotoxicity can be severe, requiring early detection and discontinuation of the drug to prevent irreversible cardiac damage [14].

Cinnamon's bioactive compounds, such as cinnamaldehyde and eugenol, exhibit strong antioxidant effects by modulating key signalling pathways involved in cellular stress responses [15]. For instance, in some *in silico* studies, it has been found that cinnamon has the potential to regulate Nrf2 (Nuclear factor erythroid 2-related factor 2) pathway and plays a crucial role in the cellular defence against the generation of oxidative stress which enhances the expression of antioxidative enzymes like catalase and superoxide dismutase (SOD) [16]. By activating the Nrf2 pathway, cinnamon can potentially help to neutralize reactive oxygen species (ROS) produced by HCQ, thereby reducing oxidative damage to cardiac cells.

Moreover, the NF-κB (nuclear factor-kappa B) signalling pathway is a key regulator of inflammation and also modulates pro-inflammatory cytokines including TNF-α (tumour necrosis factor-alpha) and IL-6 (interleukin-6), both of which are implicated in HCQ-induced cardiac inflammation [17]. Therefore, examining the potential role of cinnamon in inhibiting the NF-κB signalling pathway can reduce inflammatory cascades that would otherwise exacerbate myocardial damage. Additionally, the regulation of major apoptotic pathways, the activation of pro-apoptotic proteins and caspase signalling associated with the cardiac events taking place can be crucial to identifying the role of cinnamon when exposed to HCQ.

At the receptor level, the paradoxical interaction of HCQ with the ACE-2 receptor, which exhibits a key role in maintaining the homeostasis and normal Cardiovascular functions, causes the possibility of altering the renin-angiotensin system (RAS), causing severe cardiovascular implications or potentially worsening pre-existing cardiac anomalies. The HCQ-induced terminal glycosylation of the ACE-2 receptor leads to the imbalance and dysregulation of the ACE-

2/Ang1–7/MasR axis and may counteract the metabolic stress in cardiac cells [18]. Furthermore, cinnamon's positive effect on mitochondrial bioenergetics can help to prevent the mitochondrial dysfunction and energy depletion triggered by HCQ, potentially through modulation of the ACE-2 receptor, a master regulator of Renin-angiotensin system homeostasis.

Given the growing burden of cardiovascular diseases linked to therapeutic regimens, there is an urgent need for strategies to prevent or mitigate HCQ-induced cardiotoxicity. Therefore, in the recent study, we have identified and investigated the potential role of bioactive compounds derived from functional food, cinnamon, in attenuating the toxic effects of HCQ on the cardiovascular system and a protective effect by regulating the pro-apoptotic and inflammatory markers in the H9C2 cardiomyocyte.

MATERIALS AND METHODS

Materials and Reagents

The different analytical grade reagents and chemicals used in all the experiments were procured from Sigma. ≥99% HPLC grade of Hydroxychloroquine (H0915-5MG) powder was obtained from SIGMA; HPLC Water, Methanol and Acetonitrile (AS028-2.5L) were purchased from HIMEDIA. The filters of pore size of 0.22 µm were purchased Millipore that were used for filtration of mobile phase and sample solutions. H9C2 cardiomyocyte cell lines were purchased from NCCS, Pune (National Centre for Cell Science), India. Giemsa solution was purchased from Fisher Scientific (Prod. No. 38883). Dimethyl Sulphoxide (DMSO-67-68-5) was purchased from Qualigens, Thermo Fisher Scientific India Pvt. Ltd, Mumbai.

Collection of *C. zeylanicum* bark

The *C. zeylanicum* stem bark was collected from Noida's local market and authenticated by a botanist Dr. Anshu Rani, Department of Botany, Govt. P.G. College, Abu Road, Rajasthan, India. The barks were cleaned, air-dried, and powdered. The powder was sieved and placed in an airtight, labelled container at room temperature (28 ±2°C).

Preparation of Ethanolic Extract

10 g powder of *C. zeylanicum* bark was weighed and extraction was carried out using the Soxhlet extraction method with 95% ethanol as the solvent. Ethanol has a good solubility for organic compounds due to its low boiling point it can easily be recovered. The temperature was adjusted as per the boiling point with a 13-14 cycle run for the complete extraction of all organic compounds. After this, the use of a rotary evaporator was done to concentrate the extracts the dried mass was weighed and the percentage (%) total yield was calculated using the formula [19]:

$$Yield\ (\%) = \frac{Total\ weight\ of\ the\ solvent\ free\ extract\ (g)}{Total\ weight\ of\ the\ dried\ extract}\ X\ 100$$

Reverse Phase-High Performance Liquid Chromatography (HPLC)

At first, the process optimization was done using the different experimental sets and conditions for their different flow rate and ratios of the mobile phases. The Reverse phase HPLC analysis was performed using a Waters 1525 Binary HPLC Pump (Milford, MA, USA), equipped with a Waters 2998 Photodiode Array UV Detector (Milford, MA, USA) and a manual injector Rheodyne syringe (Trajan, Australia) of 25 µl. The Chromatogram was analysed using Empower 3 software installed on the Dell computer. The Reliant C18 5µM (4.6 X 250 mm) column was used to carry out the analysis. The separation of the sample was achieved by isocratic elution with a flow rate of 2.0 ml/min at absorbance 343 nm for 30 mins. The preparation of the mobile phase was done in the ratio of organic (Acetonitrile: Methanol – 40:60, v/v) as Solvent A and inorganic water for Solvent B with the ratio of 30:70, v/v respectively. The samples were prepared in triplicates i.e. n=3 and observed for repeatability and percentage recovery.

Fourier transform infrared spectroscopy (FTIR)

To investigate the biochemical and structural properties of the sample CZE, the FTIR was done using the Perkin Elmer Spectrum Two FT-IR Spectrometer equipped with DTGS (Deuterated triglycine sulphate) detector (model spectrum BX-II, UK) ranging from 400 to 4000 nm^{-1}. The samples were completely dried to remove the excess moisture content and were further treated with KBr which allows for the optimum transmission of Infrared light to pass through the sample during measurement.

Examination of Antiradical Activity through 2,2-diphenyl-1-picrylhydrazyl (DPPH) Assay

The DPPH scavenging activity of CZE extract was calculated by examining the extracted sample's potential to reduce DPPH into a colourless compound DPPH-H. Different concentrations of the extract ranging from 0.2 – 1 mg/ml were mixed alongwith DPPH (0.135mM) prepared in the methanol and allowed to incubate for approx. 30 min in the dark . After that, its absorbance was taken at 517 nm with a UV-VIS spectrophotometer. The antiradical scavenging potential of the extract was measured using the formula [22]-

$$Percentage\ (\%)\ Inhibition = \frac{Absorbance\ of\ the\ control - Absorbance\ of\ the\ sample}{Absorbance\ of\ the\ control}\ X\ 100$$

Maintenance of Cell Culture

The H9C2 cells derived from rat embryonic cardiomyocytes were recieved from NCCSPune,

India. The cells were then cultured in DMEM (Dulbecco's modified Eagle's Medium) which was supplemented with 10% FBS and antibiotics (penicillin and amphotericin) under the atmosphere having 5% CO_2 level and 37°C temperature to grow cells. Upon the confluency of ~70%, cells were trypsinized and seeded in a 12 and 96-well plate. HCQ drug was used to induce the stress conditions in the H9C2 cell line.

Study Groups

To observe the effects of the drug HCQ and *C. zeylanicum* extract (CZE), we divided our experimental setup into four different groups- (1) Control, where H9C2 cardiac myoblast cells were cultured without giving any treatment, (2) HCQ, drug-treated and stress-induced cells, (2) CZE, cells treated with *C. zeylanicum* ethanolic extract alone and (4) HCQ+CZE representing a combination of HCQ and CZE treatment, respectively. The control group was kept in cell culture with only DMEM media whereas the IC_{50} dose of HCQ, CZE and a combination of HCQ+CZE were calculated. The combination IC_{50} dose for HCQ and CZE was further calculated using the online software.

Cell Viability Analysis using MTT Assay in H9C2 Cell line

To measure the percentage viability of s of H9C2 cells and optimise the dose concentration for HCQ and CZE, MTT (3 -(4, 5-dimethyl-thiazol-2-yl)-2,5-diphenyl tetrazolium bromide) experiment was performed. In the initial phase, H9C2 cells were exposed to HCQ with different concentrations ranging from 10, 20, 30, 40, 50, 60, 70, 80, 90, 100 µM and CZE extract concentrations 2, 4, 6, 8, 10, 12, 14, 16,18 and 20 µg/ml for 24, 48 and 72 h compared to the control group treated with only DMEM media. Then, MTT (5 mg/ml) dissolved in PBS (Phosphate Buffer Saline) was mixed to each well and was incubated at 37°C for 3 h. The violet-coloured crystals are formed when MTT gets reduced by the activity of naturally occurring enzymes within live cells.. After this, DMSO was added to each well and was incubated for 15-20 mins in complete dark to solubilize all the formazan crystals formed. The absorbance of each well was examined with an ELISA reader (Bio-Rad) at a wavelength of 570 nm and the percentage (%) cell viability was calculated by using the formula [20] –

$$Percentage\ Cell\ Viability\ (\%) = \frac{Abs\ of\ Test - Abs\ of\ Blank}{Abs\ of\ Control - Abs\ of\ Blank}\ X\ 100$$

After calculating individual IC_{50} doses, cells were treated in a combination dose of HCQ and CZE at a constant ratio in triplicates. The combination IC_{50} was further determined to calculate the Dose reduction index (DRI) and Combination Index (CI).

***In vitro* Drug Combination Analysis**

To elucidate the dose-response relationship for quantitating the synergistic effects and combinational interaction among HCQ and CZE, we used the online software CompuSyn, which uses a Java web tool to identify the IC_{50} values. By calculating the CI (Combination Index), the synergistic and antagonistic interaction was determined in H9C2 Cardiomyoblast cell lines. After the 48 hr treatment of cells with the mixture of the individual IC_{50} values of HCQ and CZE in a fixed ratio, cell viability was determined and a dose-effective graph was plotted by combining the fractional cytotoxic impact of HCQ and CZE on the values between 0 (cell death) to 1 (No cell death).

For further validation of the CompuSyn results, Combenefit software was used to analyze the isobologram and synergism detection.

Morphological Analysis of H9C2 Cells

To study the stress-induced cellular anomalies, H9C2 cells were subjected to the treatment of HCQ and CZE, individually and in combination. An Olympus inverted microscope with 20X magnification was used to visualize the cellular morphology, a typical characteristic of cardiac stress.

Giemsa Staining of Cells

Cellular morphological changes in response to given doses were assessed using Giemsa staining in a time-dependent manner for 6, 24, 48 and 72 hr. At first, H9C2 cells were washed thoroughly, with 1X PBS and fixed using methanol (prechilled) for 15 to 20 mins. After fixation, the cells were stained with a 10% Giemsa solution for 15 to 20 mins at 25°C. Visualisation was performed at 20X magnification using an inverted microscope, allowing for detailed observation of cellular morphology [21].

Intracellular ROS Detection by DCFH-DA

2′,7′-dichlorofluorescin diacetate (DCFH-DA) staining was done to analyze the level of intracellular reactive oxygen species (ROS) in the experimental set. For this, the cells were fixed by prechilled 100% methanol after removal of the DMEM media, followed by incubation with 0.01M of DCFH-DA for 1 hour at a temperature of 37 °C followed by washing. The results were observed using a fluorescent microscope (Olympus), using a FITC filter at magnification 40X to visualise the same. The net fluorescence was then detected in the stained cells and read through a spectrofluorometer at excitation wavelength 490 nm and emission wavelength 520 nm .

Hoescht and MitoTracker Red Dual Staining

The Hoescht Stain Solution (SIGMA) method detects the blue fluorescence from the DNA of the live cells whereas MitoTracker Red CMXRos is a cell membrane permeable dye that emits red fluorescence. After seeding H9C2 cells in a 6-well plate with DMEM media, the cells were treated with doses of HCQ and CZE with the calculated doses in a different

experimental group. After 48 hrs treatment, media was removed and the cells were fixed by 100% chilled methanol followed by incubation with 8.1 µM Hoescht stain solution and 1 µM MitoTracker Red CMXRos for 30-35 mins incubation, respectively. Any extra bound Hoescht and MitoTracker Red dye was washed. After this, the cells were visualized under the fluorescent microscope at 40X magnification using a DAPI filter.

Ethidium Bromide/Acridine Orange (EtBr/AO) Dual Staining

EtBr and AO double staining method allows for the assessment of the viable cells and plays a crucial role in testing the compound and its toxicological effects. Initially, thecells were seeded and then cultured in a 12-well plate with complete DMEM media. After the incubation for 24 hrs and 48 hrs of treatment with HCQ and CZE individually and in combination, the cells were trypsinized and pelleted down. The pellet was washed two times with 1X PBS and was resuspended in 20µl of dye mixture (100 µg/ml AO and100 µg/ml EtBr) prepared in PBS. After 10 mins, 10µl of cells from each set were placed carefully on a clean glass slide with a cover slip to avoid any bubbles. The slides were then observed under a fluorescent microscope using a FITC filter with magnification 40X to visualize the cells.

Cell Apoptosis Assay: Analysis of Cell Viability and Death using Flow cytometry

Next to examine the effect of HCQ on apoptosis and cell death in the H9C2 cell line, the Muse Annexin V & Dead Cell (Luminex Corporation, U.S.A.) experiment was conducted as per the user's guide and the instructions of the manufacturer. The Muse Annexin V & Dead Cell assay allows for the *in vitro* quantitative analysis and detection of live, early and late apoptosis and cell death by utilizing Annexin V as the marker to detect phosphatidyl serine on the external surface of apoptotic cells. Briefly, 1 x 10^5 H9C2 cells were cultured in a 6-well plate and exposed to HCQ and CZE individually and in combination with the calculated IC_{50} dose for 48 hrs. The cells were collected and washed with PBS two times. A 100µl of Muse Annexin V & Dead cell reagent was carefully added to each sample. After the incubation for 20 mins at room temperature, cell analysis was done using Guava Muse Cell Analyzer (Luminex).

Statistical Analysis

All the experiments performed were repeated thrice in triplicates. The Data obtained is presented as mean ± SD. The statistical analysis has been performed using one-way analysis of variance (ANOVA) and has been evaluated using a T-test where $p<0.05$ is considered statistically significant. The IC_{50} value was obtained using the appropriate concentration inhibitory curves and plotted data is expressed on the representative graph.

Results

The extraction of bioactive compounds from 10 g of *C. zeylanicum* bark in an ethanolic medium showed good yield oily textured and a brown-coloured extract (Fig 1). The solubility of phytoconstituents in 95% ethanol generated a 37.87% yield in the total percentage extraction (Table 1). The study was initially started with the screening of the phytochemicals present in the ethanolic *C. zeylanicum* bark extract. The HPLC characterization determines the phytocompounds present in the ethanolic extract. The chromatogram showed a total of 10 different peaks of the secondary metabolites present wherein cinnamaldehyde corresponds to 27.43 min retention time with a maximum area of 8676679 µV*sec and a maximum height of 1207164 µV (Fig 2). The abundant presence of flavonoids and phenolic compounds such as Coumarin, Cinnamic acid, Kaempferol, Quercetin, Epicatechin, Gallic acid, Linalool, Chlorogenic acid, and p-coumaric were found to be present in the CZE extract (Table 2).

Fig 1: The preparation of *C. zeylanicum* ethanolic bark extract (CZE)

Type of Extract	Ethanolic
Sample weight	10 g
Extraction Yield (% w/w)	37.87 ± 0.36*
Colour	Brown
Texture	Oily

The value of yield is the mean of three replicates (n=3) of the samples ± Standard deviation

*symbol represents the significant difference of p<0.05 evaluated using a T-test

Table 1: Extraction yield of the organic extract prepared of *C. zeylanicum*

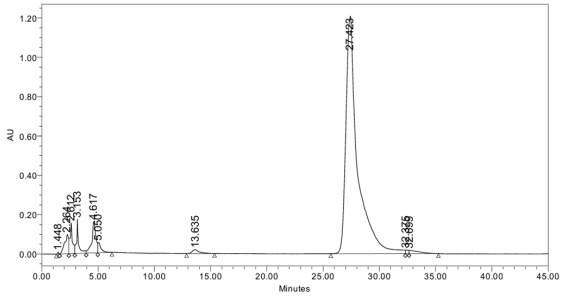

Fig 2: HPLC Chromatogram of *C. zeylanicum* ethanolic extract

Peak No.	Compounds	Retention Time (min)	Area (µV*sec)	% Area	Height (µV)
1	Chlorogenic acid	1.448	49173	0.05	9593
2	Linalool	2.264	2321852	2.30	97898
3	Gallic acid	2.612	2379546	2.36	155473
4	p-Coumaric	3.153	2110386	2.09	173713
5	Quercetin	4.617	3905679	3.87	158999
6	Epicatechin	5.050	1046944	1.04	52345
7	Coumarin	13.635	856700	0.85	19002
8	Cinnamaldehyde	27.423	8676679	86.04	1207164
9	Kaempferol	32.375	339304	0.34	18052
10	Cinnamic acid	32.699	1063377	1.05	16320

Table 2: Determination of *C. zeylanicum* ethanolic bark extract compounds with their corresponding retention time, area and height of the peak which is generated from the analysis of chromatogram

To validate the HPLC findings, we further examined the presence of functional groups present in the bioactive compounds through FTIR analysis (Fig 3). Identification and quantification of bioactive compounds play a crucial role in determining the antioxidative and anti-inflammatory potential of the phytocompound. FTIR spectrum revealed a broad band of hydroxyl group depicting alcohol by the peak at 3367 cm^{-1}. In contrast, a sharp and clear band at 2925 cm^{-1} shows the presence of the C-H group of alkanes in the sample, 1729 cm^{-1} peak confirms the presence of aldehyde with C=O group, 1676 cm^{-1} peak indicates C=C alkene group, 1452 cm^{-1} refers to the presence of aromatic compounds,1370 cm^{-1} for C-H alkanes, 1278 cm^{-1} of C-N for amines in the sample,1123 cm^{-1} acids or esters and 740 cm^{-1} relates to *cis* C-H aromatic bending as (Table 3). The strong peak C=O of aldehyde stretch vibration confirms the presence of cinnamaldehyde in the extract.

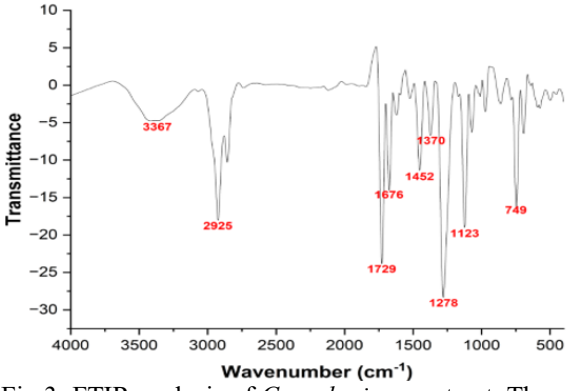

Fig 3: FTIR analysis of *C. zeylanicum* extract. The x-axis represents the wavenumber cm^{-1} of the corresponding functional groups obtained to their respective Transmittance on the y-axis

Wavenumber (cm^{-1})	Bond Type	Vibration Mode	Functional Group
3367	O-H	Stretching	Alcohol
2925	C-H	Stretching	Alkane
1729	C=O	Stretching	Aldehyde
1676	C=C	Bending	Alkene
1452	C=C	Stretching	Aromatic
1370	C-H	Bending	Alkane
1278	C-N	Stretching	Amine group
1123	C-O, C=C and C-C-O	Stretching	Acids or Esters
740	*cis* C-H	Aromatic C-H bending	Aromatic

Table 3: FTIR spectra peaks positions, mode of vibration and recognized functional groups of ethanolic extract of *C. zeylanicum*

We further verified the determined bioactive compound potential found in *C. zeylanicum* to scavenge the free radical generated due to stress conditions using DPPH assay. We found a strong antioxidative potential (40-63%) at the given increasing concentrations (0.2 -1 mg/ml) as compared to that of ascorbic acid which was used as a standard with the same increasing concentrations and showed 72- 91% free radical scavenging activity increase in CZE extract as compared to the ascorbic acid (Fig 4).

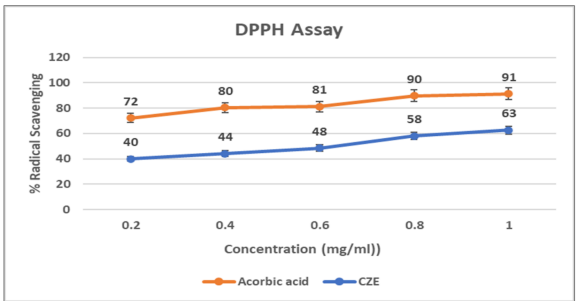

Fig 4: The DPPH graphical representation depicts 63% to be the highest scavenging potential of the extract at 1 mg/ml concentration concerning that of the Ascorbic acid at 91%

After the confirmation and quantitation of the phytocompounds enriched cinnamon extract, we further optimised the dose of HCQ and CZE alone by observing the viability of H9C2 cells using an MTT assay. The results obtained from the MTT cell viability assay showed that HCQ and CZE have time and dose-dependent effects on the H9C2 cell line after the subsequent treatment of 24 hr, 48 hr and 72 hr with the varying doses. At 48 hrs after treatment with HCQ, a concentration above 30 µg/ml showed the cell viability below 50% whereas after 72 hrs, a concentration above 15 µg/ml was considered toxic. Additionally, during 24 hrs treatment with HCQ, the cell viability for all concentrations was above 50% except 45 and 50 µg/ml. (Fig 5a and 5c). Similarly, for CZE after 48 hr treatment, H9C2 cell viability reduced below 50% at the concentration of 10 µg/ml and after 72 hr, the toxicity for the cells was reported at a concentration of 8 µg/ml. After 24 hrs of CZE treatment, a significant ($p<0.005$) decline in cell viability was observed only for 16, 18 and 20 µg/ml of CZE concentration. Therefore, 48 hr treatment given to cells was optimized and considered relevant for further analysis. Similarly, based on the most commonly used linear regression analysis, we plotted an Inhibitor vs response curve with variable slope (four parameters) (Fig 5b and 5d). The IC_{50} values of HCQ and CZE were calculated using the same. The HCQ had an IC50 value of 68.28 µM± 3 with a goodness of fit 3 and the

CZE with an IC50 value of 9.41µg/ml ± 0.85 with a goodness of fit 0.85 ($p<0.05$) was obtained. These IC_{50} doses were further used for the induction and treatment of the cardiac cells.

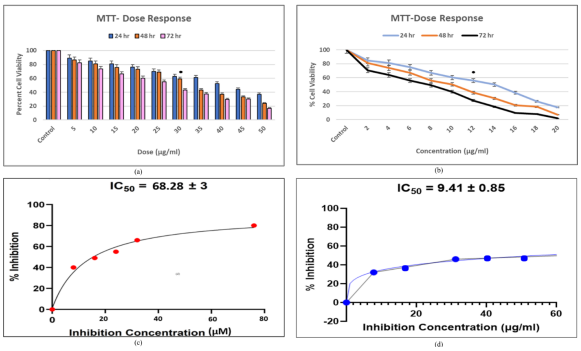

Fig 5: The MTT assay for dose optimization and IC_{50} calculation for HCQ and CZE in H9C2 cells (a) MTT dose-response graph of HCQ reveals the higher dose value for 48 hr treatment as compared to that of 28 and 78 hr, respectively (b) MTT dose-response graph curve for *C. zeylanicum* CZE extract (c) IC_{50} concentration calculation and plotting of the graph indicating 68.28 ± 3 µM as the calculated dose for HCQ (d) IC_{50} concentration calculation and plotting of the graph indicating 9.41 ± 0.85 µg/ml as the calculated dose for CZE

To further optimize the combination dose for HCQ+CZE, the cells were treated with different concentrations of HCQ+CZE for 48 hr and their combination analysis was done by mixing them in a constant ratio of their corresponding IC_{50} dose. We observed the DRI value for the drugs obtained was 3.02 ($p<0.05$) which is greater than 1 which signifies the prominence of combined dosage as compared to individual dose (Fig 6). Further validation using Combenefit isobologram evaluation confirmed the results of CompuSyn findings by showing a significant difference in the synergistic effect when given in combination therapy to the cells at a constant ratio. The selected model used was the HSA (highest single agent) model which is a dose-dependent model of synergism to quantify the stronger combinations as compared to individuals. The doses between 30 µM to 75 µM of HCQ and 10 µg/ml to 25 µg/ml of CZE (blue colour in the 3D surface plot and Contour map) confirmed the synergism in the H9C2 Cardiomyoblast (Fig 7).

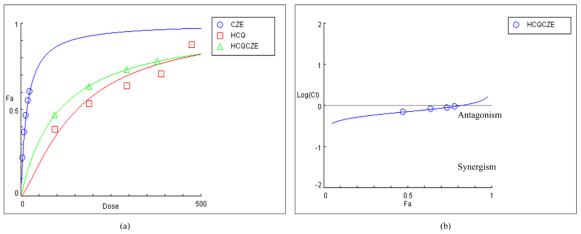

Fig 6: The combined effect of HCQ and CZE on the H9C2 Cardiomyoblast cell viability. (a) the dose-effect curve obtained with different concentrations of constant ratio for individual HCQ and CZE and in combination (b) Plot of Combination Index for H9C2 cells for different concentrations of the HCQ and CZE in combination showing the synergism where Fa value <1 ($p<0.05$)

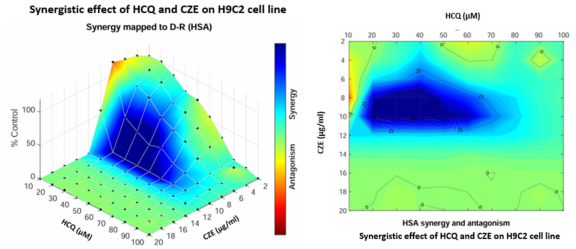

Fig 7: Confirmation of synergism and Isobologram analysis for the combination dose of HCQ and CZE in different experimental groups (n=3) using Combenefit software. (a) The 3D surface plot represents the synergism and antagonism exhibited by the combinatorial dose in blue color (b) Contour mapping of the dose in 2D analysis

We further analyzed the *in-vitro* potential of *C. zeylanicum* ethanolic bark extract. We initiated from the optimized IC_{50} doses with four experimental sets of Control, HCQ, CZE and HCQ+CZE. Since the morphology of the cells exhibits a characteristic feature in response to the stress condition, we examined the morphological changes in the H9C2 cell line in a time-dependent manner using Giemsa staining with the IC_{50} doses of the HCQ and CZE alone and in combination. For 6 and 24 hr treatment, cells exhibited the normal morphology under the CZE and Control group whereas HCQ-treated cells showed a distinct morphology with a little increased cell size. For 48 hr treatment of dose, HCQ-induced cells showed the hypertrophic condition when treated individually at 68.28 µM while CZE in combination with HCQ significantly ($p<0.05$) decreased the cell size as compared to the control (Fig 8). The cell size observed for CZE-treated cells was very similar to that of the control. After 72 hr treatment of HCQ, the cells appeared to be distorted with the uneven cellular membrane and no nuclear membrane which may further induce the cell death. The CZE-treated group and control group were very similar but with a small increase in cell size.

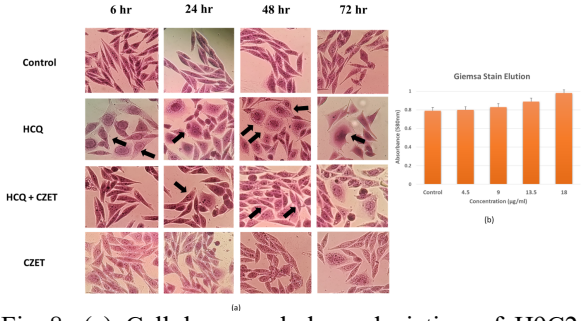

Fig 8: (a) Cellular morphology depiction of H9C2 cardiomyoblasts at 6, 24, 48 and 72 hr for the different experimental groups (Control, HCQ alone, HCQ +CZE, and CZE alone, (b) Quantification of the eluted Giemsa dye

Further to observe the imbalance in intracellular ROS generated in response to HCQ-mediated stress, DCFH-DA staining was performed. The amount of ROS produced in HCQ-treated cells with the calculated IC_{50} 63.28 µM emitted more green signals and irregular cell size and structure whereas when treated in combination with HCQ+CZE shows a significant reduction ($p<0.05$) in cell size and decreased production of ROS contributing to less green signals emitted which is comparable to that of control. Comparingly, CZE alone exhibited a significant decrease in intracellular free radical scavenging activity in cell line (Fig 9).

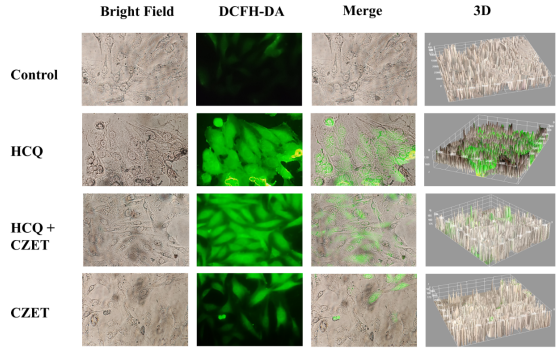

Fig 9: DCFH-DA stained images to measure the intracellular ROS detection in H9C2 cells with individual treatment of HCQ and CZE along with the combination of HCQ+CZE at their calculated IC_{50} doses. The images were quantified using ImageJ software

To visualize the cells with nuclei and to observe the changes in the production of the mROS (mitochondrial ROS), we performed the Hoescht and MitoTracker Red dual staining method. In the control group, no visible red fluorescence from MitoTracker red was observed which indicates the absence of mROS generation (Fig 10). However, intense red fluorescence with irregular and distorted nuclei in the HCQ alone treated group was detected, intensifying the increase in the production of mROS due to the stress mechanism. Interestingly, the red fluorescence was found to decrease in the cells with combination treatment of HCQ + CZE. This demonstrates the reversal or mitigation of the stress caused by the drug HCQ when taken individually. The CZE alone cells were very similar to that of the control group with normal cellular integrity and mitochondrial function.

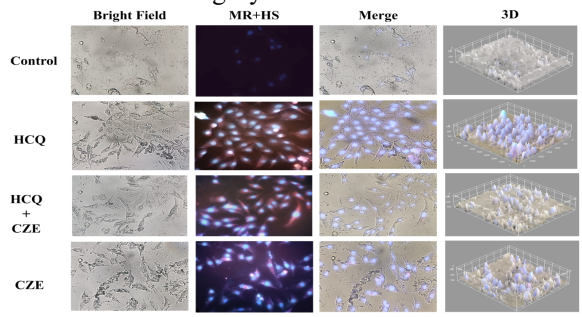

Fig 10: Nuclear integrity and mROS detection by Hoescht (HS) and MitoTracker Red (MR) dual staining analysis H9C2 cells with individual treatment of HCQ and CZE along with the combination of HCQ+CZE at their calculated IC_{50} doses. The images were quantified using ImageJ software

Apoptosis due to the production of oxidative stress and excessive ROS production induced in the cells was examined using EtBr/AO dual staining method. We examined the experimental sets under the fluorescent microscope. The uniform distribution of light green colour confirmed no significant apoptosis in the cells of the control group (Fig 11a). In the HCQ-treated cells, distribution of uneven fluorescence of red-orange with the peripheral increase and disintegration of the cells was observed (Fig 11b). The early to late apoptotic stage was detected and marked with the yellow-green fluorescence by AO in an early apoptotic stage which is concentrated to one side of the cell giving a crescent or granular appearance of the H9C2 cells and biased orange fluorescence of the nucleus by EtBr which is either partially dissolved or near about the disintegration (Fig 11c). The cells treated with CZE show slight green fluorescence, much similar to the control group (Fig 11d).

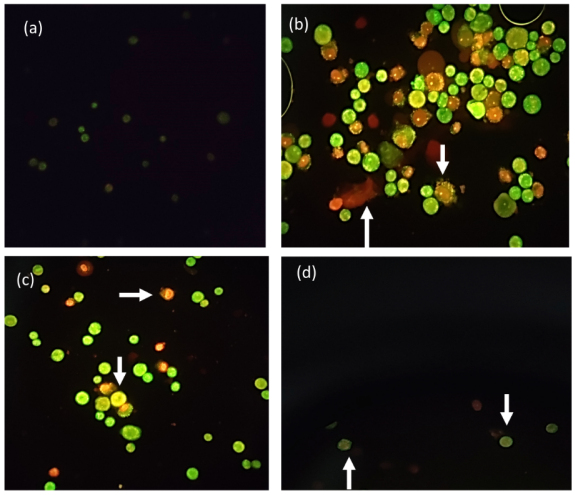

Fig 11: Examination of the EtBr/AO double staining under the fluorescence microscope. (a) Control: Light green in color (nucleus uniformly distributed in center); (b) HCQ treated (Necrotic cells): Uneven orange-red fluorescence either dissolved or near disintegration; (c) CZET: Light Yellow-green fluorescence by AO concentrated at one side; and (d) HCQ + CZET (early - Late apoptotic cells): Nucleus orange fluorescence bias spread by EtBr either dissolved or near disintegration

To validate the apoptosis stages, we performed the flow cytometric assessment using Muse Annexin V & Dead Cell analysis. When the H9C2 cell lines were treated with 68.28 µM HCQ resulted in 46.45% total apoptosis (23.40% early and 23.05% late apoptosis) compared to 1.30% of necrosis. Interestingly, the co-treatment of 68.28 µM HCQ and 9.41 µg/ml CZE, significantly ($p<0.05$) reduced total apoptosis by 25.75% (21.90% early and 3.85% late apoptosis) with 73.85% live cells. Notably, a substantial difference was seen in necrosis with 0.40% cell death observed when given in combination. Moreover, when 9.41 µg/ml CZE was given individually, 80.50% of live cells and 19.50% total apoptosis (19.50% early and 0% late apoptosis) was seen which is much comparable to the control group with 4.8% total apoptosis (4.8% early and 0.8% late apoptosis) and 95.20% live cells and no cell death was seen (Fig 12). The population profile of the experimental sets also validates the findings of Muse Annexin V & Dead Cell assay (Fig 13).

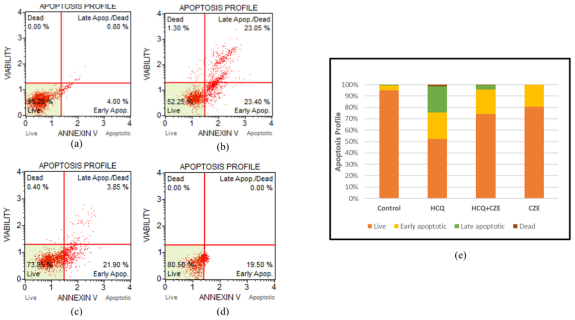

Fig 12: The Flow cytometry analysis of Annexin V and Dead Cell kit by Muse cell Analyzer. H9C2 cells were treated with different doses of (a) Control group; (b) HCQ alone, (c) CZE alone and (d) HCQ+CZE combination, respectively. The Four quadrants show, Upper left – Dead cells, Upper right – Late apoptotic cells, Lower left – Live cells and Lower right – Early apoptotic cells

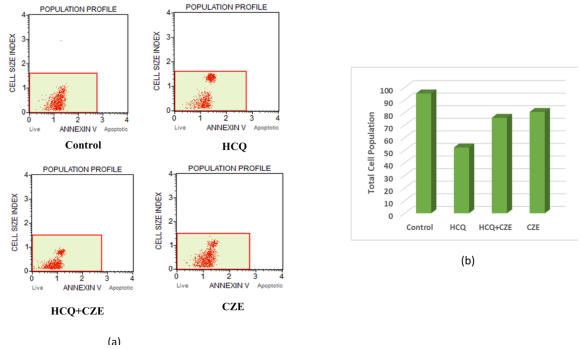

Fig 13: (a) The total cell population profile of Control, HCQ treated, HCQ+CZE combination treated and CZE alone treated groups (b) Graphical representation of population profile

Discussion

The synergistic effect of HCQ+CZE on the molecular and cellular mechanism of HCQ-induced toxicity on Cardiac cells has not been well documented. The results obtained from our current study demonstrate the mitigation of HCQ-generated stress in H9C2 cardiac myocytes.

The increasing evidence of cardiovascular complications associated with long-term drug use is a global health concern [22]. The current COVID-19 epidemic has increased the prescription and usage of the repurposed drug HCQ [23]. Recent research demonstrates that chronic HCQ usage could trigger the formation of oxidative stress and ROS, which can further lead to arrhythmias, hypertension, and serious cardiac problems [24]. Thus, increased oxidative stress can lead to apoptosis and cell death in cardiac cells, eventually leading to heart failure [25]. We observed the significant increase in cell size and hypertrophy associated with the treatment of HCQ to cardiac cells compared to the healthy cells exhibiting distinct morphology characterised by specific size, shape and

integrity. Giemsa staining confirmed the increase in cell size and distorted morphology in HCQ-treated cells. An imbalance in the generation of intracellular ROS and antioxidants in the cells treated with HCQ contributes to oxidative stress. Increased levels of oxidative stress contribute to mitochondrial dysfunction and impaired mitochondrial ROS generation [26]. Moreover, the generation of oxidative stress can potentially induce nuclear deformation indicative of cellular dysfunction [27]. Our results from Hoescht-Mitored dual staining validated the generation of mROS and distorted nuclei due to the HCQ-induced stress mechanism in cardiac cells. Similarly, in healthy conditions cells have intact cell membranes acting as selective barriers which prevent the entry of certain molecules whereas in damaged or compromised cells membrane allows them to enter indicating the cellular injury [28]. Moreover, stress-induced conditions often disrupt the delicate balance between antioxidant formation and ROS generation, which can ultimately trigger apoptotic cell death [29]. Our study confirmed the disturbances in the cell membrane permeability and intracellular distribution of apoptotic markers in HCQ-induced cells thereby providing valuable insights into the stage of apoptosis (early or late) using EtBr/AO dual staining method.

C. zeylanicum has been known to have promising therapeutic potential for improving human health and well-being [30]. The bioactive compounds present in cinnamon possess anti-inflammatory and antioxidant properties that can contribute to the prevention and management of chronic diseases and organ toxicity [31]. Here, we examined the potential of cinnamon-derived bioactive compounds to mitigate the cardiovascular toxicity of HCQ by regulating pro-apoptotic and inflammatory markers in H9C2 cardiomyocytes. Phytochemical screening validates the abundance of hydroxyl groups of flavonoids and phenols in the *C. zeylanicum* extract. The increased consumption of foods rich in polyphenols and flavonoids such as epigallocatechin, quercetin, kaempferol, etc. has the potential to reduce oxidative cellular damage, tissue inflammation, DNA damage, and cardiovascular diseases [32]. Evidence from studies showed that flavonoids could regulate oxidative stress and inflammatory response through anti-inflammatory mechanisms targeting the pathways like NF-κB signalling mechanism [33].

Free radical production contributes to the occurrence of several types of chronic diseases, including cardiovascular disease and the development of cancer [34]. Antioxidants play a crucial role in counteracting their adverse effects by reducing the generation of free radicals inside the body [35,36,37]. In the present study, CZE has shown a good capacity to scavenge any free radicals generated via stress or imbalance in an increasing concentration.

To investigate the potential of *C. zeylanicum* in HCQ-induced toxicity, we performed the comparative study using combined IC_{50} doses of 68.28 µM and 9.41 µg/ml of HCQ and *C. zeylanicum* treatment. Interestingly, our findings revealed the reduction in the toxicity by HCQ in a time-dependent manner. The staining images confirmed the findings obtained as the H9C2 cells appear to be in a more uniform and clear structure compared to that of hypertrophic condition when treated with HCQ alone.

Imbalance in ROS generation leads to oxidative stress contributing to the development of hypertension, heart disease and atherosclerosis[38,39]. Our study shows a significant reduction ($p<0.05$) in cell size and decreased production of ROS contributing to less green signals emitted when treated with combined dose through DCFH-DA staining. This clearly shows the antioxidative potential of *C. zeylanicum* in mitigating the ROS generated by HCQ. Therefore, this study validates the *C. zeylanicum* bioactive's potential as a cardioprotective agent by reducing the oxidative stress in the cardiovascular system. The study was further validated by Hoescht and MitoTracker Red dual staining where the red fluorescence was found to decrease in the cells mROS with combination treatment of HCQ + CZE. This demonstrates the reversal or mitigation of the stress caused by the drug HCQ when taken individually.

The production of ROS can promote apoptosis by controlling the proliferation of multiple networks of anti-apoptotic or pro-apoptotic protein molecules, such as the caspases [40]. Apoptosis is mediated by the cascade of two major events via early apoptosis which involves degradation of mitochondrial membrane potential and activation of caspases whereas late apoptosis is rrestricted by the fragmentation of DNA, formation of apoptotic bodies and nuclear collapse[41,42,43]. Late apoptosis is generally initiated by the uncleared early apoptotic cellular events [44]. Experimental evidence suggest that targeting the early apoptotic pathway can potentially prevent the cells from entering late apoptosis and mitigate the negative consequences associated with excessive apoptosis [45]. By inhibiting the progression of late apoptosis, it may be possible to reduce the generation of ROS thereby contributing to the cells' damage and necrosis [46]. In our study, examination of EtBr/AO staining of cardiac cells reveals the reversal of cells in late apoptosis to early apoptosis conditions. These results obtained were validated using Flow cytometric analysis. In HCQ+CZE co-treated cells 23.40% of early apoptotic cells increases to 25.75% early apoptosis with 3.85% late apoptosis. Notably, a substantial difference was seen in necrosis

with 0.40% cell death observed when given in combination. The findings demonstrate necrosis which ultimately leads to apoptosis is the primary pathway through which HCQ exerts cytotoxic effects on H9C2 cardiomyoblasts. Moreover, the decrease in late apoptosis suggests the cytoprotective potential of CZE in preventing the progression of early apoptosis and reducing late apoptosis, thereby decreasing the overall stress conditions in the cells. Additionally, the reduction of necrosis in combination with CZE also plays an important role in mitigating the progression towards necrosis and cell death which further supports the cardioprotective role of *C. zeylanicum* against HCQ-induced toxicity.

Conclusion

The findings of the study elucidate the substantial cytotoxic effects of the repurposed drug HCQ on the H9C2 cardiomyoblasts cells primarily through inducing oxidative stress and apoptosis. The prolonged administration of HCQ potentially results in a pronounced increase in both late and early apoptosis confirming that apoptosis is the main mechanism of cell death and necrosis. However, the synergistic treatment with ethanolic extract of *C. zeylanicum* significantly attenuated the HCQ-induced apoptotic response, inhibiting late apoptosis and necrosis progression. This reduction in the mechanism of apoptosis and cellular stress can be due to the abundant bioactive compounds such as phenols, flavonoids, and cinnamaldehyde present in functional food which helps to mitigate oxidative stress and enhance cellular viability. In addition, the presence of antioxidants in *C. zeylanicum* reinforces its therapeutic potential in counteracting HCQ-induced toxicity and promoting cell survival.

Overall, our research investigations support the antioxidative potential of *C. zeylanicum* as a potential functional food and natural therapeutic agent to mitigate the adverse effects of drug-induced cellular stress, oxidative damage and toxicity.

Future Prospects

Further research is needed to explore the molecular pathways through which phytoconstituents-rich *C. zeylanicum* exerts its cytoprotective effects with the main focus to study its interaction with the intra and inter-cellular signalling pathways involved in the apoptosis mechanism. *In-vivo* studies could reveal a better understanding of the cardioprotective role of *C. zeylanicum* under long-term exposure to the drug HCQ and its potential to mitigate cardiotoxicity in clinical settings. Additionally, the optimization of dose for combination strategies of *C. zeylanicum* with other drugs also will enhance its therapeutic efficacy. Investigation for future studies to identify the potential of Cinnamon as a nutraceutical in counteracting oxidative stress-related disorders, metabolic disorders and cardiovascular diseases with its promising antioxidant profile could strongly provide a deep dive into its therapeutic relevance.

Acknowledgements

We acknowledge Jaypee Institute of Information and Technology, Noida, India for providing infrastructure and literature support.

Statements and Declarations

Ethical Approval

Not Applicable

Consent to Participate

Not Applicable

Consent to Publish

Not Applicable

Authors Contributions

Priyadarshini Gupta: Writing-original draft, Writing-Review & editing, Methodology, Visualization.

Vibha Rani: Resources**,** Conceptualization**,** Writing-Review & editing, Supervision.

Competing Interests

The authors have no relevant financial or non-financial interests to disclose.

Availability of data and materials

Not Applicable

Conflict of Interest

The authors declare that they have no conflict of interest.

Code availability

Not Applicable

Funding

The research was supported by the DST-INSPIRE grant awarded to Ms Priyadarshini Gupta (DST/INSPIRE Fellowship/2019/IF190735; Mentor: Prof. Vibha Rani) and ICMR grant awarded to Prof. Vibha Rani (67/4/2022-DDI/BMS)

References

1. Dua, S., Sahrawat, N. & Chaturvedi, N. Encapsulation: A Revolutionary Approach to Preserving Bioactive Compounds in Functional Food Products. Reson 29, 541–556 (2024).
2. Arumugam, Vignesh & Thomas Cheeran, Amal & Ariyan, Sarvalingam & Vasanth, Krishnan. (2024). A Review on the Influence of Nutraceuticals and Functional Foods on Health. Food Chemistry Advances. 5.
3. Patel, K.R., Chahwala, F.D., Yadav, U.C.S. (2018). Flavonoids as Functional Food. In: Rani, V., Yadav, U. (eds) Functional Food and Human Health. Springer, Singapore.
4. Rana, P., Lee, MS. & Sheu, SC. Authentication of Cinnamomum verum (Ceylon cinnamon) in commercial products by qualitative and real-time quantitative PCR assays. Eur Food Res Technol (2024).

5. Cena H, Calder PC. Defining a Healthy Diet: Evidence for The Role of Contemporary Dietary Patterns in Health and Disease. Nutrients. 2020 Jan 27;12(2):334.
6. Singh AK, Pal P, Pandey B, Goksen G, Sahoo UK, Lorenzo JM, Sarangi PK. Development of "Smart Foods" for health by nanoencapsulation: Novel technologies and challenges. Food Chem X. 2023 Oct 4;20:100910.
7. Eidi, A., Mortazavi, P., Bazargan, M., & Zaringhalam, J. (2012). Hepatoprotective activity of cinnamon ethanolic extract against CCI4-induced liver injury in rats. EXCLI journal, 11, 495–507.
8. Lei ZN, Wu ZX, Dong S, Yang DH, Zhang L, Ke Z, Zou C, Chen ZS. Chloroquine and hydroxychloroquine in the treatment of malaria and repurposing in treating COVID-19. Pharmacol Ther. 2020 Dec;216:107672.
9. Jaeger A, Sauder P, Kopferschmitt J, Flesch F. Clinical features and management of poisoning due to antimalarial drugs. Med Toxicol Adverse Drug Exp. 1987 Jul-Aug;2(4):242-73.
10. Gupta P, Rani V. The Surging Mechanistic Role of Angiotensin Converting Enzyme 2 in Human Pathologies: A Potential Approach for Herbal Therapeutics. Curr Drug Targets. 2023;24(13):1046-1054.
11. Melles RB, Marmor MF. The risk of toxic retinopathy in patients on long-term hydroxychloroquine therapy. JAMA Ophthalmol. 2014 Dec;132(12):1453-60.
12. Wu Q, Ross AJ, Ipek T, Thompson GH, Johnson RD, Wu C, Camelliti P. Hydroxychloroquine and azithromycin alter the contractility of living porcine heart slices. Front Pharmacol. 2023 May 5;14:1127388.
13. Stokkermans TJ, Falkowitz DM, Trichonas G. Chloroquine and Hydroxychloroquine Toxicity. [Updated 2024 Jan 11]. In: StatPearls [Internet]. Treasure Island (FL): StatPearls Publishing; 2024 Jan-.
14. Gupta, P., Rani, V. A Comprehensive Assessment of Environmental Implications, Ecotoxicity and Bioaccumulation Potential of Repurposed Drug Hydroxychloroquine: From Challenges to Sustainability. Reviews Env.Contamination (formerly:Residue Reviews) 262, 10 (2024).
15. Aggarwal, S., Bhadana, K., Singh, B., Rawat, M., Mohammad, T., Al-Keridis, L. A., Alshammari, N., Hassan, M. I., & Das, S. N. (2022). Cinnamomum zeylanicum Extract and its Bioactive Component Cinnamaldehyde Show Anti-Tumor Effects via Inhibition of Multiple Cellular Pathways. Frontiers in pharmacology, 13, 918479.
16. Khedkar, S., & Ahmad Khan, M. (2023). Aqueous Extract of Cinnamon (Cinnamomum spp.): Role in Cancer and Inflammation. Evidence-based complementary and alternative medicine : eCAM, 2023, 5467342.
17. Velikova TV, Kabakchieva PP, Assyov YS, Georgiev TA. Targeting Inflammatory Cytokines to Improve Type 2 Diabetes Control. Biomed Res Int. 2021 Sep 13;2021:7297419.
18. Chen, L., Chen, H., Dong, S., Huang, W., Chen, L., Wei, Y., Shi, L., Li, J., Zhu, F., Zhu, Z., Wang, Y., Lv, X., Yu, X., Li, H., Wei, W., Zhang, K., Zhu, L., Qu, C., Hong, J., Hu, C., … Hao, G. (2020). The Effects of Chloroquine and Hydroxychloroquine on ACE2-Related Coronavirus Pathology and the Cardiovascular System: An Evidence-Based Review. Function (Oxford, England), 1(2), zqaa012.
19. Abbas A, Naqvi SAR, Rasool MH, Noureen A, Mubarik MS, Tareen RB. Phytochemical Analysis, Antioxidant and Antimicrobial Screening of Seriphidium Oliverianum Plant Extracts. Dose Response. 2021 Mar 30;19(1):15593258211004739.
20. Isa, H. I., Ferreira, G. C. H., Crafford, J. E., & Botha, C. J. (2019). Epoxyscillirosidine Induced Cytotoxicity and Ultrastructural Changes in a Rat Embryonic Cardiomyocyte (H9c2) Cell Line. Toxins, 11(5), 284.
21. Deepthi, B., Prayaga, A. K., & Rukmangadha, N. (2022). Comparison of Modified Ultrafast Giemsa Stain with the Standard May Grunwald Giemsa Stain in FNAC of Various Organs. Journal of cytology, 39(4), 174–179.
22. Gagnon LR, Sadasivan C, Perera K, Oudit GY. Cardiac Complications of Common Drugs of Abuse: Pharmacology, Toxicology, and Management. Can J Cardiol. 2022 Sep;38(9):1331-1341.
23. Zhou, G., de Vos, S., Schuiling-Veninga, C. C. M., Bos, J., Oude Rengerink, K., Pasmooij, A. M. G., Mol, P. G. M., de Bock, G. H., & Hak, E. (2023). Community Use of Repurposed Drugs Before and During COVID-19 Pandemic in the Netherlands: An Interrupted Time-Series Analysis. Clinical epidemiology, 15, 923–937.
24. Rezabakhsh, A., Montazersaheb, S., Nabat, E., Hassanpour, M., Montaseri, A.,

Malekinejad, H., Movassaghpour, A. A., Rahbarghazi, R., & Garjani, A. (2017). Effect of hydroxychloroquine on oxidative/nitrosative status and angiogenesis in endothelial cells under high glucose condition. BioImpacts : BI, 7(4), 219–226.
25. De Geest, B., & Mishra, M. (2021). Role of Oxidative Stress in Heart Failure: Insights from Gene Transfer Studies. Biomedicines, 9(11), 1645.
26. Peoples, J.N., Saraf, A., Ghazal, N. et al. Mitochondrial dysfunction and oxidative stress in heart disease. Exp Mol Med 51, 1–13 (2019).
27. Cui T, Lan Y, Lu Y, Yu F, Lin S, Fu Y, Qiu J, Niu G. Isoorientin ameliorates H_2O_2-induced apoptosis and oxidative stress in chondrocytes by regulating MAPK and PI3K/Akt pathways. Aging (Albany NY). 2023 Jun 5;15(11):4861-4874.
28. Rizzuto R, De Stefani D, Raffaello A, Mammucari C. Mitochondria as sensors and regulators of calcium signalling. Nat Rev Mol Cell Biol. 2012 Sep;13(9):566-78.
29. Villalpando-Rodriguez, G. E., & Gibson, S. B. (2021). Reactive Oxygen Species (ROS) Regulates Different Types of Cell Death by Acting as a Rheostat. Oxidative medicine and cellular longevity, 2021, 9912436.
30. Wang, Y. C., Wang, V., & Chen, B. H. (2023). Analysis of bioactive compounds in cinnamon leaves and preparation of nanoemulsion and byproducts for improving Parkinson's disease in rats. Frontiers in nutrition, 10, 1229192.
31. Ho YS, Wu JY, Chang CY. A New Natural Antioxidant Biomaterial from Cinnamomum osmophloeum Kanehira Leaves Represses Melanogenesis and Protects against DNA Damage. Antioxidants (Basel). 2019 Oct 11;8(10):474.
32. Rudrapal M, Khairnar SJ, Khan J, Dukhyil AB, Ansari MA, Alomary MN, Alshabrmi FM, Palai S, Deb PK, Devi R. Dietary Polyphenols and Their Role in Oxidative Stress-Induced Human Diseases: Insights Into Protective Effects, Antioxidant Potentials and Mechanism(s) of Action. Front Pharmacol. 2022 Feb 14;13:806470.
33. Mahboob A, Senevirathne DKL, Paul P, Nabi F, Khan RH, Chaari A. An investigation into the potential action of polyphenols against human Islet Amyloid Polypeptide aggregation in type 2 diabetes. Int J Biol Macromol. 2023 Jan 15;225:318-350.
34. Khodayar, M. J., Kalantari, H., Mahdavinia, M., Khorsandi, L., Alboghobeish, S., Samimi, A., … Zeidooni, L. (2018). Protective effect of naringin against BPA-induced cardiotoxicity through prevention of oxidative stress in male Wistar rats. Drug and Chemical Toxicology, 43(1), 85–95.
35. Jena AB, Samal RR, Bhol NK, Duttaroy AK. Cellular Red-Ox system in health and disease: The latest update. Biomed Pharmacother. 2023 Jun;162:114606.
36. Atale N, Gupta K, Rani V. Protective effect of Syzygium cumini against pesticide-induced cardiotoxicity. Environ Sci Pollut Res Int. 2014;21(13):7956-72.
37. Atale N, Mishra CB, Kohli S, Mongre RK, Prakash A, Kumari S, Yadav UCS, Jeon R, Rani V. Anti-inflammatory Effects of S. cumini Seed Extract on Gelatinase-B (MMP-9) Regulation against Hyperglycemic Cardiomyocyte Stress. Oxid Med Cell Longev. 2021 Mar 3;2021:8839479. doi: 10.1155/2021/8839479.
38. Yan, Q., Liu, S., Sun, Y. et al. Targeting oxidative stress as a preventive and therapeutic approach for cardiovascular disease. J Transl Med 21, 519 (2023).
39. Atale, N., Chakraborty, M., Mohanty, S. et al. Cardioprotective Role of Syzygium cumini Against Glucose-Induced Oxidative Stress in H9C2 Cardiac Myocytes. Cardiovasc Toxicol 13, 278–289 (2013).
40. Li M, Wang D, He J, Chen L, Li H. Bcl-X_L: A multifunctional anti-apoptotic protein. Pharmacol Res. 2020 Jan;151:104547.
41. Fuchs Y, Steller H. Live to die another way: modes of programmed cell death and the signals emanating from dying cells. Nat Rev Mol Cell Biol. 2015 Jun;16(6):329-44.
42. Madeo F, Fröhlich E, Fröhlich KU. A yeast mutant showing diagnostic markers of early and late apoptosis. J Cell Biol. 1997 Nov 3;139(3):729-34.
43. West AP, Shadel GS. Mitochondrial DNA in innate immune responses and inflammatory pathology. Nat Rev Immunol. 2017 Jun;17(6):363-375.
44. Suroto H, Asriel A, De Vega B, Samijo SK. Early and late apoptosis protein expression (Bcl-2, BAX and p53) in traumatic brachial plexus injury. J Musculoskelet Neuronal Interact. 2021 Dec 1;21(4):528-532.
45. Patel, V. A., Longacre, A., Hsiao, K., Fan, H., Meng, F., Mitchell, J. E., Rauch, J., Ucker, D. S., & Levine, J. S. (2006). Apoptotic cells, at

all stages of the death process, trigger characteristic signaling events that are divergent from and dominant over those triggered by necrotic cells: Implications for the delayed clearance model of autoimmunity. The Journal of biological chemistry, 281(8), 4663–4670.

46. Jeong, C. H., & Joo, S. H. (2016). Downregulation of Reactive Oxygen Species in Apoptosis. Journal of cancer prevention, 21(1), 13–20.